EARTH SURFACE PROCESSES AND LANDFORMS
Earth Surf. Process. Landforms **44**, 417–432 (2019)

Published online 31 October 2018 in Wiley Online Library
(wileyonlinelibrary.com) DOI: 10.1002/esp.4504

Effects of estuarine mudflat formation on tidal prism and large-scale morphology in experiments

Lisanne Braat,* **Jasper R. F. W. Leuven,** **Ivar R. Lokhorst and Maarten G. Kleinhans**
Department of Physical Geography, Faculty of Geosciences, Utrecht University, Utrecht, The Netherlands

Received 28 March 2018; Revised 27 August 2018; Accepted 10 September 2018

*Correspondence to: Lisanne Braat, Department of Physical Geography, Faculty of Geosciences, Utrecht University, Utrecht, The Netherlands. E-mail: L.Braat@uu.nl

ESPL
Earth Surface Processes and Landforms

ABSTRACT: Human interference in estuaries has led to increasing problems of mud, such as hyper-turbidity with adverse ecological effects and siltation of navigation channels and harbours. To deal with this mud sustainably, it is important to understand its long-term effects on the morphology and dynamics of estuaries. The aim of this study is to understand how mud affects the morphological evolution of estuaries. We focus on the effects of fluvial mud supply on the spatial distribution of mudflats and on how this influences estuary width, depth, surface area and dynamics over time. Three physical experiments with self-forming channels and shoals were conducted in a new flume type suitable for tidal experiments: the Metronome. In two of the experiments, we added nutshell grains as mud simulant, which is transported in suspension. Time-lapse images of every tidal cycle and digital elevation models for every 500 cycles were analysed for the three experiments. Mud settles in distinct locations, forming mudflats on bars and sides of the estuary, where the bed elevation is higher. Two important effects of mud were observed: the first is the slight cohesiveness of mud that causes stability on bars limiting vertical erosion, although the bank erosion rate by migrating channels is unaffected. Secondly, mud fills inactive areas and deposits at higher elevations up to the high-water level and therefore decreases the tidal prism. These combined effects cause a decrease in dynamics in the estuary and lead to near-equilibrium planforms that are smaller in volume and especially narrower upstream, with increased bar heights and no channel deepening. This trend is in contrast to channel deepening in rivers by muddier floodplain formation. These results imply large consequences for long-term morphodynamics in estuaries that become muddier due to management practices, which deteriorate ecological quality of intertidal habitats but may create potential area for marshes. © 2018 The Authors. Earth Surface Processes and Landforms Published by John Wiley & Sons Ltd.

KEYWORDS: estuary morphodynamics; mudflat; tidal prism; flume experiments; shoal accretion

Introduction

Estuaries are tidally influenced coastal bodies of water that are connected to a river system supplying fresh water and sediments. Estuaries occur in a wide variety of planform shapes and shoal patterns, which are caused by inherited initial conditions and changing boundary conditions. However, it is still unclear how these conditions contribute to the evolution of estuaries and therefore a full understanding of their behaviour is still lacking. Understanding these natural dynamics is relevant for ecology, economy and flood safety, since intertidal areas are important ecological habitats and estuaries often have important shipping fairways to inland harbours that are located in densely populated areas. Many estuaries are heavily managed to balance these values, but there is a need to increase our understanding of the natural dynamics to improve management strategies.

Alluvial estuaries are typically flanked by mudflats and salt marshes (Dalrymple *et al.*, 1992; Dalrymple and Choi, 2007). Mud has different erosional and depositional characteristics from sand and can, therefore, affect the morphology of estuaries. Recently, interest in estuarine mud has increased, because many estuaries have been dealing with increased negative effects of mud (e.g. fluid mud, siltation of channels and harbours, higher turbidity reducing light penetration, attraction of pollutants; Ridgway and Shimmield, 2002; Dijkstra *et al.*, 2011; Van Maren *et al.*, 2015, 2016). On the positive side, mudflats are very productive areas for flora and fauna, though vulnerable because of their low biodiversity (Costanza *et al.*, 1993). Only very few studies consider the decadal to centennial effects of mud on the morphology of the estuary. Studying these long-term trends might give better insights into more sustainable or more efficient management strategies, and prediction of long-term morphological behaviour may improve by accounting for mud. For example, if we can determine how tidal channels migrate over time in relation to the amount of cohesive mud in the system, we can perhaps better manage causes of hyper-turbidity and dredge more sustainably by migrating the shipping route in accordance with the natural trend of the estuary.

Previous research on the long-term morphodynamics of estuaries has mostly been conducted by numerical modelling (e.g. Lanzoni and Seminara, 2002; Hibma *et al.*, 2003; Van der Wegen and Roelvink, 2008, 2012; Van der Wegen

et al., 2008; Moore *et al.*, 2009; Van der Wegen, 2013; Dam *et al.*, 2016; Braat *et al.*, 2017), whereas only few studies use physical experiments (Reynolds, 1887, 1889, 1891). Also, long-term field data are scarce and limited to decades rather than centuries. For such long timescales, only numerical modelling studies are available, but these may suffer from weaknesses such as neglected processes, numerical effects, imperfect transport predictors and the need for calibration of physics-based parameters (Baar *et al.*, 2018). Additionally, these studies rarely include mud because this has only become possible very recently (Le Hir *et al.*, 2001; Van Kessel *et al.*, 2011; Dam *et al.*, 2013; Braat *et al.*, 2017). Therefore, complementary to numerical models, additional approaches are necessary, such as physical models that form the entire landscape on scale within one flume.

Experiments with self-forming estuaries are rare, especially compared to the large number of delta experiments (e.g. Smith, 1909; Hoyal and Sheets, 2009; Grimaud *et al.*, 2017), meandering river experiments (e.g. Friedkin, 1945; Tal and Paola, 2007; Braudrick *et al.*, 2009; Van Dijk *et al.*, 2013) and braided river experiments (e.g. Ashmore, 1991), and even compared to the few tidal channel and inlets experiments (Tambroni *et al.*, 2005; Stefanon *et al.*, 2010; Vlaswinkel and Cantelli, 2011; Kleinhans *et al.*, 2015). Physical experiments with lightweight sediment have been conducted for filling of deltas and river floodplain (e.g. Peakall *et al.*, 2007; Van Dijk *et al.*, 2013; Hoyal and Sheets, 2009). Peakall *et al.* (2007) describe the necessity of cohesive fines in experiments to maintain a meandering planform. This was later explained by two effects: Braudrick *et al.* (2009) found that filling of floodplain by suspended sediment reduces the tendency to form chute cut-offs that are the onset of braiding. Van Dijk *et al.* (2013) found that adding cohesive sediment reduced erosion rates and increased bank strength, while overbank sedimentation and lateral accretion on point bars led to a reduction in chute cut-offs. The resulting reduction of width-to-depth ratio reduces the tendency to braid and leads to alternate bars associated with the onset of meandering. Hoyal and Sheets (2009) found that cohesive deltas show stronger channelisation, narrow channels, slower channel migration rates and therefore a more complex coastline. With these results in mind, we hypothesise that cohesive sediment deposits in estuaries will also reduce the tendency to form new channels, increase bank strength and limit the migration of channels similar to rivers and deltas.

The objective of this study is to identify the effects of cohesive sediment supply on the shape and development of estuaries. We specifically focus on the effect on large-scale parameters that determine landward tidal penetration, bar pattern and large-scale dynamics, such as width, depth and depth distribution, surface area, volume and cumulative erosion and deposition over time.

Methods

The results presented in this paper are derived from three experiments. The initial and boundary conditions of these experiments were based on the experience gained from 35 exploratory experiments with varying initial and boundary conditions. In the three experiments that are presented here, we changed the cohesive sediment supply to systematically explore the effects of this changing boundary condition. In this paper we will present an experiment with *only sand*, an experiment with a *low mud supply* and an experiment with a *high mud supply*. The experiment with only sand is also presented in Leuven *et al.* (2018a), where estuaries with growing forced tidal bars are shown to determine a non-ideal estuary planform, which serves as a reference experiment for this study.

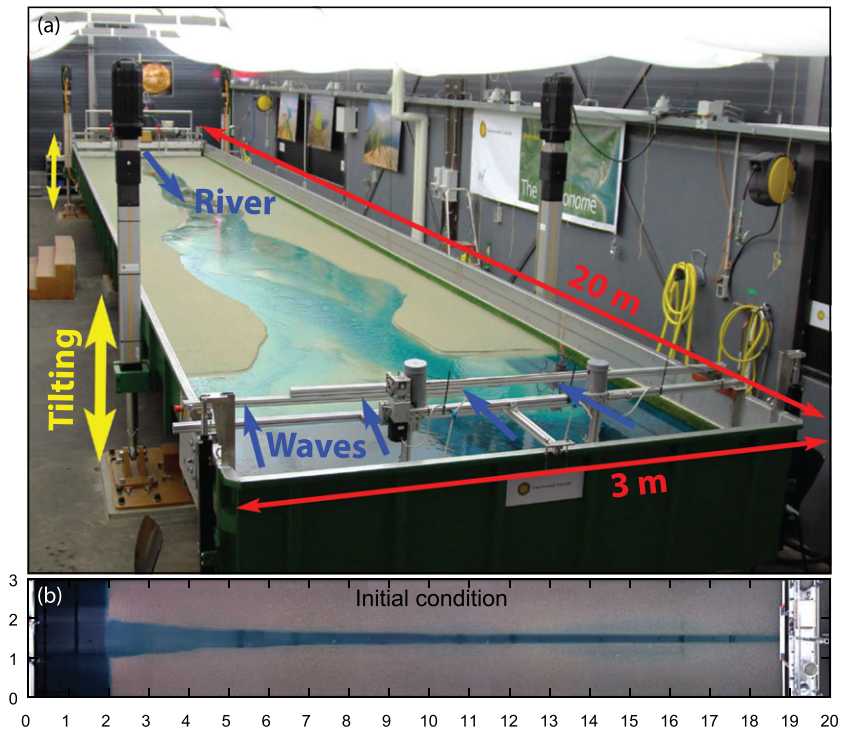

Figure 1. The Metronome: (a) the flume drives the flow by periodic tilting of the entire 20 × 3 m flume. Upstream input is river discharge and mud and downstream waves are generated; (b) overhead imagery of the initial conditions, with estuary mouth on the left and river on the right. [Colour figure can be viewed at wileyonlinelibrary.com]

Experimental set-up and scaling

The experiments are conducted in a recently built flume – the Metronome – of 20 × 3 m in size, which drives tidal flow by periodic tilting of the entire flume (Figure 1; Kleinhans *et al.*, 2017b). Until now, it has always been difficult to study estuaries with physical models (Hughes, 1993; Kleinhans *et al.*, 2012), due to scaling problems caused by tidal flow in addition to general scaling issues (Paola *et al.*, 2009; Kleinhans *et al.*, 2014a). Older tidal experiments without the periodic tilting mechanism had a tendency to exclusively form ebb-dominated, sediment-exporting systems (as reviewed in Kleinhans *et al.*, 2012). Furthermore, these experiments suffered from low sediment mobility, and bar-forming tendencies were often overwhelmed by a significant number of scour holes and small bedforms, probably due to hydraulic smooth conditions (Kleinhans *et al.*, 2017a). The recently developed Metronome flume prevents these scaling issues by obtaining appropriate hydraulic similarity and sediment mobility, and therefore sediment transport similarity, in agreement with proven scaling methods that are required to obtain morphological similarity (Peakall *et al.*, 1996; Paola *et al.*, 2009; Kleinhans *et al.*, 2014a). In particular, we solved a classic scaling conflict between sediment friction and sediment mobility by using a coarse sediment to prevent hydraulic smooth conditions and associated scour holes (Kleinhans *et al.*, 2017a), and at the same time increasing the Shields mobility number to similar values to those found in nature by driving the periodic flow by periodic flume tilting 2017b, as explained in detail below. Pilot set-ups of this system have already been used in studies on tidal basins and ebb- and flood-dominant channels (Kleinhans *et al.*, 2012, 2014b, 2015), and the Metronome has also already been proven to be a more effective method of producing dynamic estuaries compared to solely vertical water fluctuations (Kleinhans *et al.*, 2017b; Leuven *et al.*, 2018a). Previous morphodynamic experiments showed that tidal bars scale similarly to tidal bars in natural systems: the length-to-width ratio and their correlation with local estuary width is in accordance with natural systems (Leuven *et al.*, 2018a). However, the formation of cohesive tidal flats flanking non-cohesive channels within one experiment is novel in the experiments presented here.

The most important scale issue is that of sediment mobility. In scale experiments where the spatial dimensions of the system are reduced, the sediment often has a similar grain size as in nature, while the water depth is much smaller, leading to a lower velocity and therefore lower sediment mobility. If sediment is scaled down similarly to water depth the physicochemical sediment properties would change; sand would become strongly cohesive clay. Therefore, it is common practice in river experiments to increase the slope of the flume to counteract the unscaled grain size to create realistic sediment mobility and as a result realistic transport rates (Peakall *et al.*, 1996; Kleinhans, 2010). The problem in tidal experiments is that water and sediment should be transported in two directions and therefore an increased slope would only favour ebb-related transport. By using the novel tilting method of the Metronome, this is avoided. During ebb flow, the flume is tilted seaward, whereas during flood the flume is tilted landward. With this method we obtain peak Shields numbers of 0.15–0.2 for sand, which is well above the beginning of motion and close to that of small natural estuaries, obtaining sediment transport similarity while maintaining subcritical flow (Kleinhans *et al.*, 2017b). In theory, decreasing the density of the sediment is also a possibility to reduce most of these scaling issues. However, using, for example, plastic sediment is unfavourable for experiments with mud or vegetation and leads to practical problems of cost and waste treatment. The tilting method is based on several pilot studies in smaller flumes (Kleinhans *et al.*, 2012, 2014b, 2015), and a more extensive description, operation and technical information of the flume can be found in Kleinhans *et al.* (2017b).

Boundary and initial conditions

The tilting amplitude of the metronome is 75 mm, resulting in a maximum slope of 0.0075 mm^{-1} (or 0.75%) and tilts with a period of 40 s for the experiments with only sand and the experiment with a high mud supply. The experiment with a low mud supply was subjected to a slightly lower tilting amplitude of 68 mm, but the same period. Tilting amplitude and period were chosen so that sediment mobility was ensured for correct scaling, and the tidal excursion length was shorter than the length of the flume (see Kleinhans *et al.*, 2017b, for description and comparison to natural systems). These values for tilting amplitude and period were chosen on the basis of pilot tests with a range of tilting amplitudes and periods (see supplementary Figures S1 and S2, provided as supporting information, for the results of these pilots). The mean water level was set 0.065 m above the flume floor and −0.005 m elevation relative to the land surface. The resulting water-level amplitude of the experiments is 0.5–1 cm, which is less than half the typical water depth of 3 cm, a similar ratio to natural systems (Savenije, 2015). Upstream we add a river discharge of 300 $L\,h^{-1}$ during ebb, and downstream we generate waves with a paddle during flood with a frequency of 2 Hz and 1 cm amplitude (supplement of Leuven *et al.*, 2018a). The river discharge alone is not strong enough to transport sand in the flume in absence of tilting (supplementary Figure S3b). However, when tilting is applied without river discharge, a closed, short tidal basin develops (supplementary Figure S3c), showing that a minor river discharge is essential to develop an elongated estuary. The experiment starts with a bed thickness of 7 cm that consists of only sand, with an exponential widening shape of 3 cm deep (Figure 1, bottom). The initial shape decreases from 1 m width at the mouth of the estuary to 0.2 m at the river end, with a characteristic e-folding convergence length of 3 m. The bottom of the flume is covered with artificial grass. If scours develop that reach the bottom of the flume, the roughness of the grass prevents further erosion in this location. The basin area in which the ebb delta can expand during the experiment is 2 m long. Water levels in the flume are controlled by a weir at the end of the flume, while pumps constantly add water to the sea basin. This weir compensates for the tilting of the flume by maintaining a horizontal water level (constant head) in the sea between the end of the flume and the front of the ebb delta at all times. Because the ebb delta grows, the compensation of the weir is adjusted during the experiment. Water flowing out of the flume is recirculated. The total duration of each experiment is 15 000 tidal cycles.

The experiment with the low nutshell supply had a slightly lower tilting amplitude than the other two experiments. Instead of 75 mm, this experiment used a tilt of 68 mm. This was due to an accidental software update of the Metronome during the period the experiments were carried out, which was only discovered after the experiment was finished. Based on pilot studies focused on amplitude variations, we do not expect that this error influenced the main outcomes of this study. However, we expect that the resulting estuary might be slightly shorter and smaller. The effect of tilting amplitude on estuary length is indicated by pilot experiments shown in supplementary Figure S1 (supporting information). The length

of the estuaries is approximately constant throughout the experiments, in contrast to estuary width.

Sediment characteristics

To simulate mud in the experiment we used nutshell grains (as used elsewhere: Baumgardner, 2016; Ganti *et al.*, 2016; Van de Lageweg *et al.*, 2016; Baar *et al.*, 2018). Pre-wetted nutshell was added to the system during ebb with the river discharge. We conducted an experiment with a low concentration of 1 mL nutshell per cycle (0.405 $g\,L^{-1}$) and an experiment with a high concentration of 5 mL nutshell per cycle (2.025 $g\,L^{-1}$). In total, 12 kg and 60 kg of nutshell was supplied to these experiments over 15 000 cycles. However, not all nutshell deposited in the estuaries: a large part was also transported out of the estuary and settled in the ebb delta. Throughout the paper, we will refer to these experiments as experiments with *low* and *high* mud supply concentration.

The nutshell was chosen to simulate mud because it is lightweight, with a dry density of 1350 $kg\,m^{-3}$, and therefore travels in suspension, and because it is only slightly cohesive. To test the exact cohesive effect of nutshell over time, we conducted bank erodibility tests using the method of Friedkin (1945) and the exact same set-up as Van Dijk *et al.* (2013) and Kleinhans *et al.* (2014a). Sediment samples created in the lab were subjected to a flow of 400 $L\,h^{-1}$ under an angle of 45°. Pictures were made every 10 s to track the volume of the sample over time and to measure the erosion rate. The samples that were tested were 10 × 37 cm with a triangular corner cut off of 10 × 10 cm. The samples were made of a combination of 4/5 sand and 1/5 nutshell on top and were kept under similar circumstances as in the Metronome for a variable number of days. To create similar circumstances the samples were almost fully submerged with recirculating water flow with approximately the same amount of anti-algae and chlorine that was used in the Metronome. As other authors suggest, the nutshell is indeed non-cohesive if subjected to experimental conditions for only a short time (as mentioned by Ganti *et al.*, 2016). However, mud deposits became more difficult to erode due to slight decomposition over time and perhaps fungal development, as in natural estuaries where the critical shear stress for erosion increases over time due to consolidation and biofilm development (Torfs *et al.*, 1996).

Sand in the experiments has a median grain size of 0.55 mm with a D_{10} of 0.32 mm and a D_{90} of 1.2 mm (for design see Kleinhans *et al.*, 2017b). The sand mixture was prepared by wet sieving, which completely removed any fines below 0.125 mm. There was no sand supply upstream. The nutshell has a grain size of 0.2 mm. Preliminary tests with the nutshell indicated that coarse nutshell (1.3–1.7 mm) not only settles with low velocities but also deposits when the grain size is larger than the water depth on bars. We hypothesise that this effect might be the cause of the different point bar deposits for nutshell and silt in Van de Lageweg *et al.* (2016), where nutshell deposited dominantly on the downstream half of the point bar, while the silt deposited in the upstream half. A much smaller nutshell grain size was used for the estuary experiments and solved this difference between the silt and nutshell behaviour. This means that we are simulating a finer fraction than in the river experiments by Van de Lageweg *et al.* (2016).

Data collection and analysis

Time-lapse images were collected using 7 AVG Mako (G-419C) colour cameras on the ceiling. All images have a resolution of 2048 × 2048 pixels with a footprint of about 3.15 m, resulting in a pixel resolution of approximately 1.5 mm. The images were taken every tidal cycle when the bed was horizontal. Pre-processing of the images included debayering of the original Bayer images, noise removal, lens correction (vignette and distortion), geometric rectification, and colour, contrast and brightness correction, after which the images were stitched together. The water was dyed blue with food colouring to get an impression of water depth from the top-view photographs. Additional images were obtained every 500–1000 tidal cycles when we temporarily drained the experiment. This way the nutshell was classified more easily, compared to the images with water. Mud was classified per pixel based only on colour thresholds in the images without water.

A digital Canon SLR camera was used to collect oblique photos of the experiment. These photos were used to make digital elevation models (DEMs) by structure from motion software Agisoft PhotoScan (version 1.2.6.2038) and were referenced with 20 ground control points along the sides of the flume at a 2 m interval. In the analysis of the DEMs unaffected areas of the flume were masked and the ebb delta was excluded unless stated otherwise.

Particle image velocimetry (PIV) on floating plastic particles was used to obtain surface water velocities in the entire flume at 16 phases (every 22.5°) of the tidal cycle. Ten images were taken every phase with a sampling frequency of 25 Hz. The MPIV MATLAB toolbox was used to calculate the velocities from the floating particles. PIV measurements were performed every 500–1000 cycles in the experiment without nutshell up to cycle 8863 and at the end of the experiment with a low input concentration of nutshell. There are no PIV measurements during the experiments with nutshell because removal of the plastic particles influenced the mud deposits. During pre-processing of the PIV images, lens correction was done before the velocities were calculated from displacement of the particles, but geometric rectification and stitching of the velocity data from different cameras were done afterwards due to memory issues. Additionally, the tilt of the Metronome was not taken into account, but since discontinuities are barely visible in the stitched images we assumed that the projection errors were negligible.

During post-processing, the peak velocity ratio was calculated from the ratio between the maximum ebb and flood velocities. To make the colour scale more readable we took the negative reciprocal ($-1/x$) of the values between 0 and −1 so that ebb dominant would be negative and flood dominant positive. If only flood or only ebb flow was measured, no ratio was calculated and therefore plotted as zero. For example, highly elevated shoals sometimes flood and drain in the same direction, because maximum high water does not occur at exactly the same time as slack water.

Results

We will first describe the general evolution of the estuary in several phases. This is followed by an analysis of the location of mud deposits and the effects of the mud in the estuary.

General estuary evolution

The development of the experimental estuary consists of four phases. In the first phase of the experiments, the exponentially converging channel starts to develop a channel-shoal pattern. This pattern develops within approximately 100 tidal cycles, resulting in an alternate bar pattern (Figures 2a–2c). At the

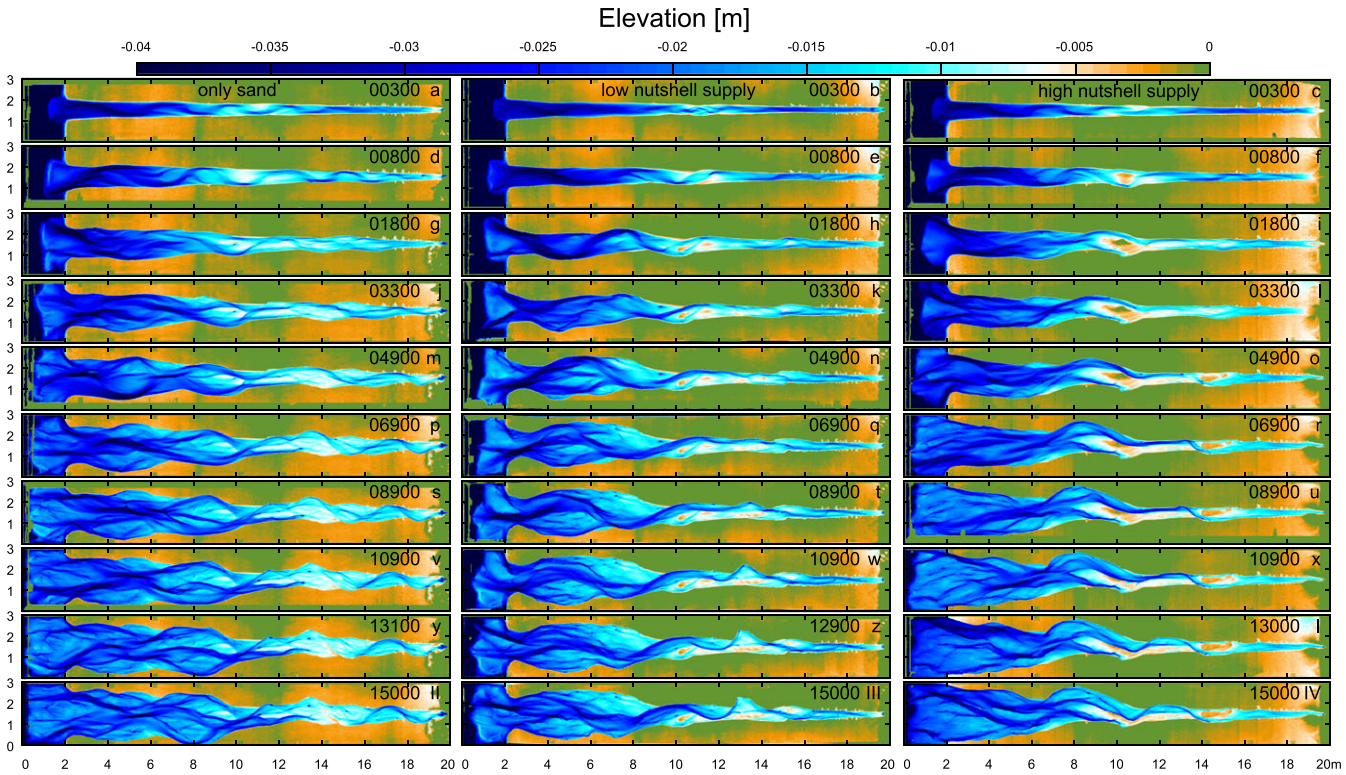

Figure 2. Time series of digital elevation models of the experiments without mud (left column), with a low mud supply (middle column) and a high mud supply (right column). [Colour figure can be viewed at wileyonlinelibrary.com]

same time, the ebb delta starts to form and continues to grow throughout the experiment. Sand is collected in the middle of the flume, caused by a lack of sediment input upstream and downstream and an estuary planform that does not exactly fit the imposed hydrodynamic conditions (Figure 3). At the end of this phase, the estuary contains one big meandering channel with sills between bends (cycle 300, Figures 2a–2c).

In the second phase, the estuary widens rapidly by outward and downstream migration of tidal meanders (Figure 4). In some places there is little lateral widening over time and, in other places, a large lateral extension of the tidal meanders. The width generally decreases in the upstream direction even though there are local areas that are wider (Leuven *et al.*, 2018a). In addition, the bed profile changes to a more linear profile by reworking of the initial bulge (Figure 3). Although there is some downstream bend migration, this is limited to the initial phase of the experiment. The widening of the estuary favours the formation of multiple channels and bars across the estuary. Small flood channels that end on bars, named barb channels, increase in size and develop into connected ebb- and flood-dominated channels (Leuven *et al.*, 2018a, cycle 800; Figures 2d–2f;). After about 1800 tidal cycles these multiple channels become clearly visible as a weakly braided pattern (Figures 2g–2i).

In the third phase from cycle 3300, the first effects of the mud are observed on the estuary width (Figures 4 and 2j–2l). The first mudflats start forming in the upper part of the estuary and slowly spread further downstream. However, they rarely settle in the lower estuary due to the large reworking of sediment in the area and constantly migrating channels and bars.

In the fourth phase and final state, the morphology after 15 000 tidal cycles for the three experiments is a self-formed, freely erodible, bar-built estuary with migrating channels and bars (Figure 2II–2IV). The experiments approach dynamic equilibrium from cycle 10 900 (Figures 2v–2x), because we see a levelling of the cumulative sedimentation and erosion (Figure 5). In the final state, the width of the estuary generally decreases in the upstream direction (Figure 4) and the bed profile increases linearly (Figure 3). The typical resulting channel depth at the mouth is 4 cm and average bed levels are 2–2.5 cm at the mouth of the estuary (Figure 3). Typical velocity amplitudes are 0.3–0.4 ms^{-1} (Figures 6 and 7), with maximum velocities occurring in the deepest channels downstream (Figure 6). However, width-averaged velocity amplitudes are lower downstream than upstream.

Mudflat characteristics

The experiments with mud supply resulted in estuaries with self-formed mudflats. The nutshell particles settle on the highest elevations of intertidal areas and form mudflats (or 'nutflats'). The mudflats occur on bars and flank the estuary (Figures 8 and 9). The flats can be recognised by an orange to brown colour which is related to the time the mud has been in the system. We observe mud deposits on all types of bars: for example, mid-channel bars (Figures 9a, 9b and 9e), scroll bars (Figure 9c) and sidebars (Figures 9d and 9e). On the bars, mud first settles at the highest locations, after which the flat spreads to lower elevations if it can grow in size.

The mud supplied upstream is self-distributed throughout the whole estuary, but mostly settles in the upstream regions (Figure 8). Initially, mud only deposits upstream, which results here in relatively high percentages of mudflats (Figure 10). For the experiment with high mud supply, the fraction upstream of 10 m after only a few hundred cycles is already approximately 40%. Over time, the mudflat area increases upstream and gradually extends more downstream as well, which is especially clear in Figure 10b, where the front between low and high percentages of mud moves downstream over time. In this experiment, a large volume of mud settles in the lower estuary, but the coverage is still less than 50% of the estuary width (Figure 10).

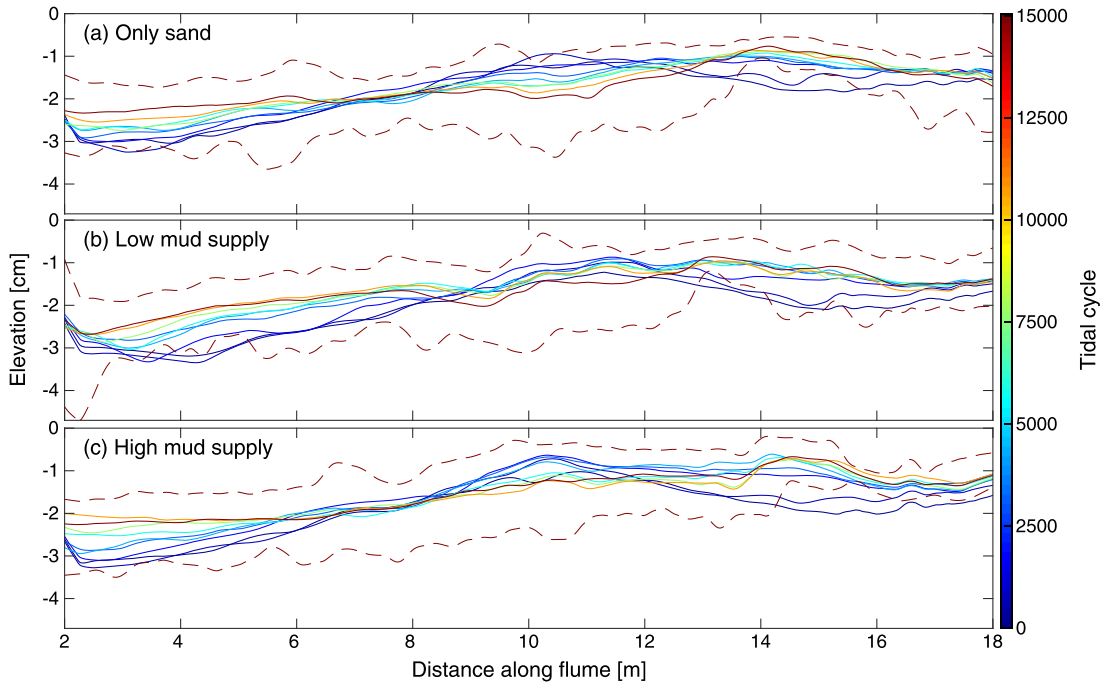

Figure 3. Mean (solid), 5 and 95 percentile (dashed) elevation along the estuary for the experiment with (a) only sand, (b) a low mud supply and (c) a high mud supply, indicating the evolution over time. Colours indicate different moments in time. The along-bed elevation was median filtered over a length of 500 pixels, which equals 0.5 m. [Colour figure can be viewed at wileyonlinelibrary.com]

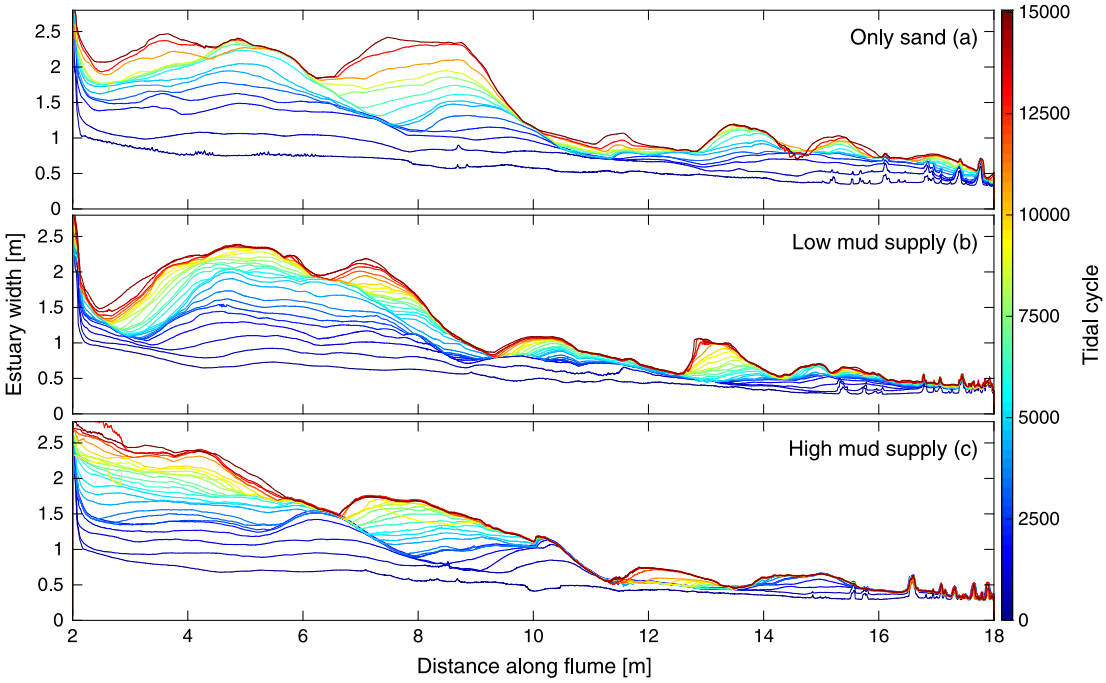

Figure 4. Width along the estuary for (a) the experiment with only sand, (b) the experiment with a low mud supply and (c) the experiment with a high mud supply. Colours indicate different moments in time. [Colour figure can be viewed at wileyonlinelibrary.com]

For the experiment with a higher mud supply, we observe that mudflats are, as expected, larger and more abundant – as high as 12.5 m^2 – compared to 3 m^2 for the experiment with low mud supply (Figure 8). Relatively, this is a mud coverage of 62% of the surface area for the experiment with high mud supply and 15% for the experiment with low mud supply, which is consistent with the fact that the high mud supply is five times larger than the low mud supply. Additionally, downstream spreading occurs faster (Figure 10). After about 8000 cycles the upstream part is so dominated by mud that it also deposits in the channels (Figure 8). This means that the relative mud cover approaches 100% (Figure 10).

Initially, mud only deposits at high elevations between −1.5 and −0.5 cm near the observed high-water level, mostly on bars (Figure 11, dotted lines). Over time, this lower knickpoint in Figure 11 (dotted lines) becomes weaker and decreases to about −2.2 cm for the highest supply. We hypothesise that this is due to different kinds of deposits later in the experiments (e.g. filling of abandoned channels). However, the majority of the mud is still located between −1.5 and −0.5 cm.

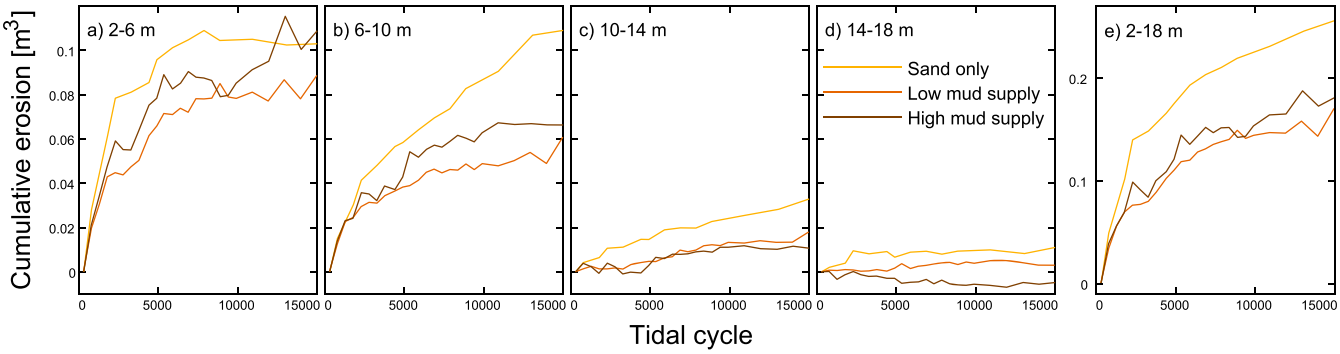

Figure 5. Cumulative sediment removed from the estuary over time for the three experiments, between (a) 2–6 m, (b) 6–10 m, (c) 10–14 m, (d) 14–18 m and (e) 2–18 m. Larger export occurred for the experiment with only sand. Experiments approach dynamic equilibrium. [Colour figure can be viewed at wileyonlinelibrary.com]

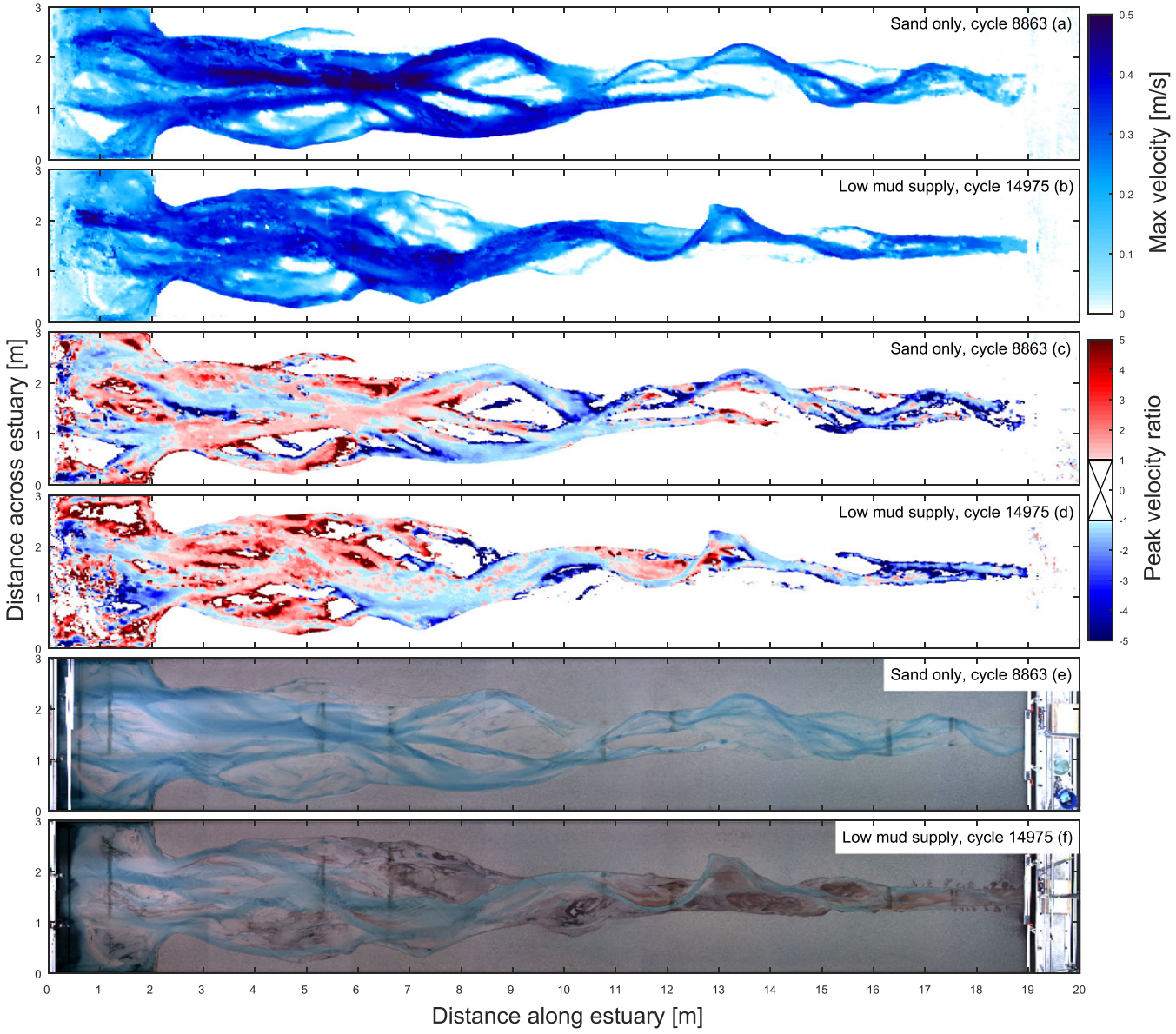

Figure 6. Maximum surface velocity over a tidal cycle for (a) sand only at cycle 8863 and (b) low mud supply at cycle 14975. Peak velocity ratio for (c) sand only at cycle 8863 and (d) low mud supply (b) at cycle 14975. Positive numbers indicate flood dominated and negative is ebb dominated. The number indicates the times the peak flood or ebb flow is larger than the flow in the other direction. No data if the flow was unidirectional or if the area was not flooded during the measurement. Related time-lapse images are shown in (e) for sand and (f) for low mud supply. [Colour figure can be viewed at wileyonlinelibrary.com]

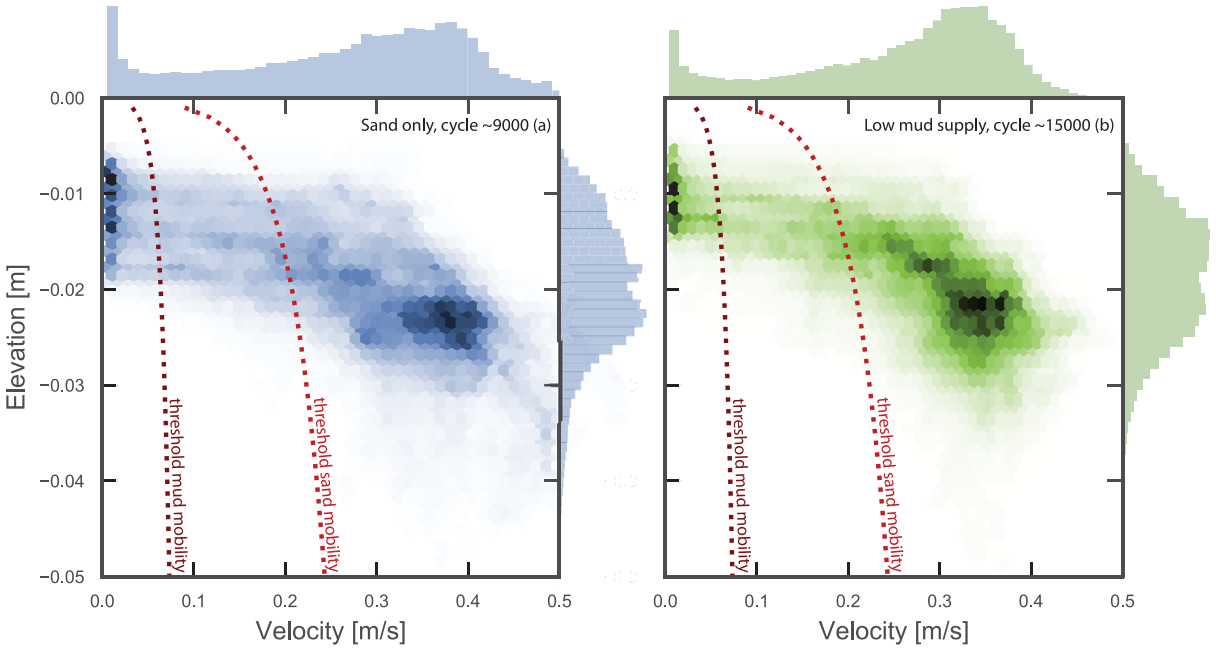

Figure 7. Scatter plot of elevation plotted against maximum surface velocity. Colour intensity and histograms at the sides indicate the velocity and elevation distribution. Still-water level is at −0.005 m. Dotted lines indicate the critical threshold of motion for sand and mud. (a) Experiments with only sand at cycle 8863; (b) experiment with low mud supply at cycle 14975. [Colour figure can be viewed at wileyonlinelibrary.com]

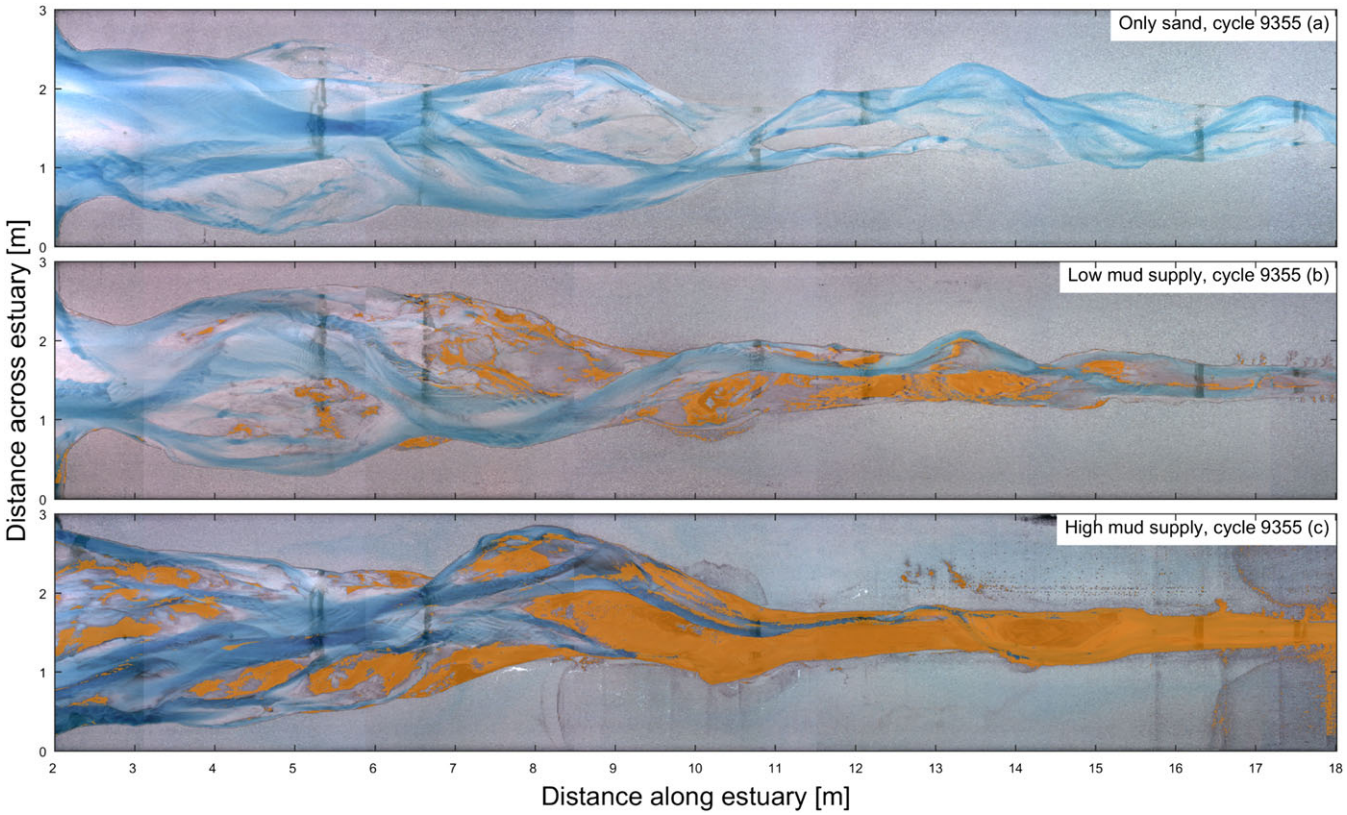

Figure 8. Spatial distribution of mud (classified in orange) in the estuary with (a) only sand, (b) a low mud supply and (c) a high mud supply at cycle 9355. [Colour figure can be viewed at wileyonlinelibrary.com]

Mud preservation

To understand which areas in the estuary are influenced most by mud, we investigated which mud deposits are most stable. The age of mud could be estimated by combining the mud maps to indicate the stability of the mudflats (Figure 12). We assume that mud was not eroded and redeposited between two images. From these data we can see that some upstream bars show a pattern: first, a small flat develops and then this mudflat expands in the upstream direction and to lower elevations. In the middle of the estuary, the mudflats are very stable in location and size, and some locations have been stable since the beginning of the experiment (for about 15 000 cycles). Downstream, the mudflats are much younger in age (about 2000 cycles) due to larger dynamics of the channels. A small remnant of old mud remained at 9 m (Figure 12a).

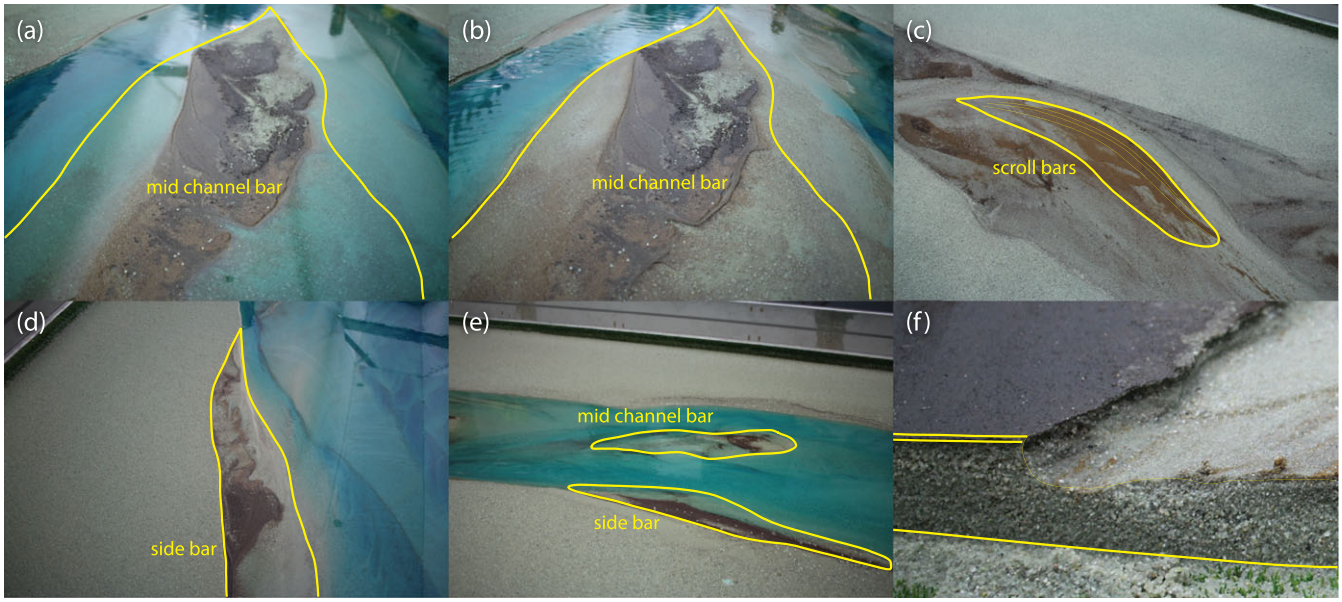

Figure 9. Detailed photographs of mud deposits in the experiments: (a) mudflat with high water; (b) mudflat with low water; (c) scroll bars; (d) mudflat on the side; (e) mudflat on a bar and on the side; and (f) cross-section of a channel with steep banks, indicating cohesive nature of the nutshell deposits. [Colour figure can be viewed at wileyonlinelibrary.com]

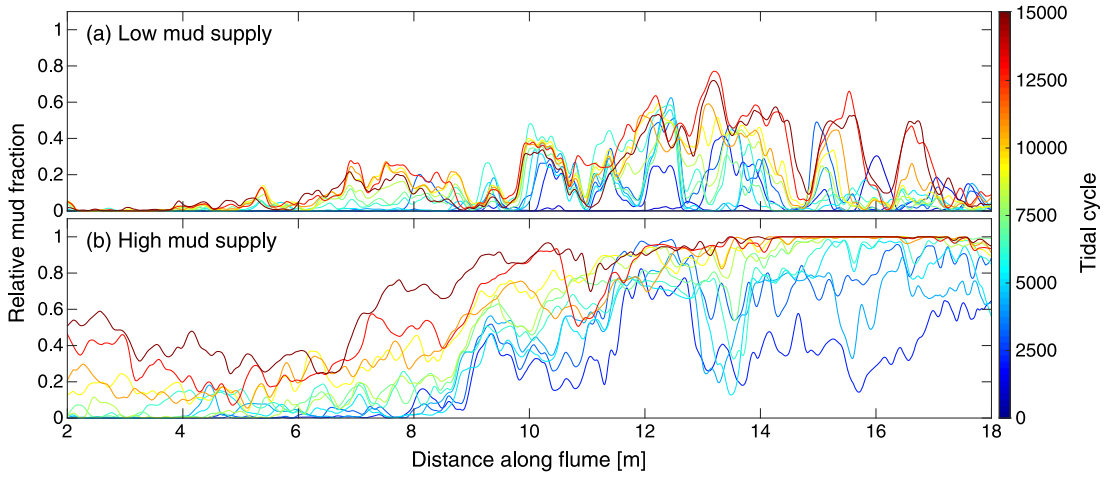

Figure 10. Mud cover relative to the estuary width along the estuary for (a) the experiment with a low mud supply and (b) the experiment with a high mud supply. Colours indicate different moments in time. The relative mud fraction was median filtered over a length of 200 pixels, which equals 0.2 m. [Colour figure can be viewed at wileyonlinelibrary.com]

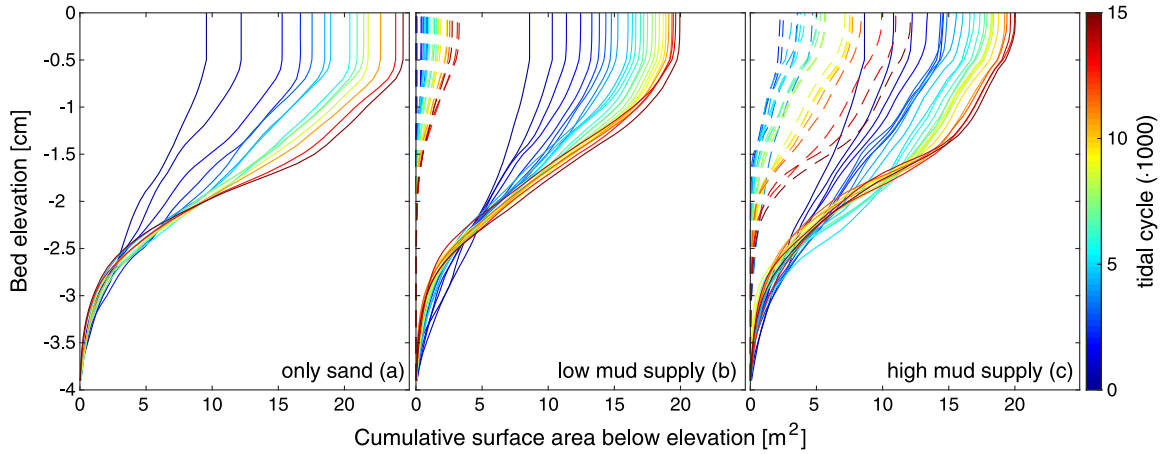

Figure 11. Cumulative total estuary area (solid) and mud-covered area (dashed) below a certain elevation for the experiment with (a) only sand, (b) a low mud supply and (c) with a high mud supply. Colours indicate different moments in time. [Colour figure can be viewed at wileyonlinelibrary.com]

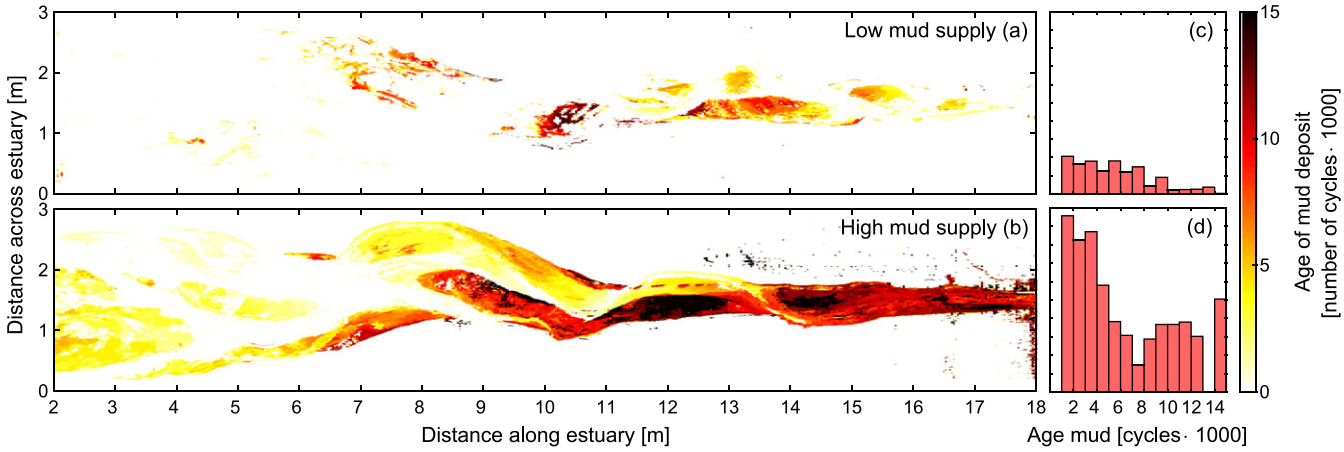

Figure 12. Spatial maps of the age of the mud deposits for the experiments with (a) a low mud supply and (b) a high mud supply. Darker colours indicate older deposits. (c, d) Histograms of maps (a, b) of mud age for the final situation. [Colour figure can be viewed at wileyonlinelibrary.com]

This is a remnant of a larger mudflat that has disappeared due to the downstream migration of the biggest channel. Other analysis showed that mud deposits initially at a lower range of elevations as well but is only preserved at high elevations for a long time since older mud deposits occur at higher elevations, which is consistent with our explanation based on velocities and water levels. This is in contrast to rivers, where mud will never deposit at larger depths due to unidirectional flow, except in closed residual channels.

The effect of mud on morphodynamics

Bank erosion and erosion rates

The channel banks showed steep cliffs at the edges of bars that were subjected to erosion, which is evidence that the nutshell has some cohesive properties. We observed preferential erosion of sand over the nutshell at the bar margins (Figure 9f). Sand was eroded from bar margins by undercutting of the mud layer on top of the flat, after which the mud eroded by small collapses. This is in contrast to the gentler sloping sandy bar margins.

The Friedkin (1945) erosion tests were used to determine the exact effect of the mud on bank erosion. In this case, it behaves as non-cohesive, lightweight sediment as, for example, plastic sediments that are transported more easily than sand. However, when we added a thin mud layer on top of a sand sample, we observe that after several days the grains stick together and form a mat. This mat becomes stronger over time and changes the erosion mechanism of the samples. Instead of slumping sand, we now observe oversteepening and collapsing (as in Figure 9f).

Despite this difference, there were no significant differences in the erosion rate of the samples with and without mud layer and between different sample times (Figure 13). Cohesive blocks that end up at the toe of the bank by collapses are immediately removed due to excess basal capacity as observed in similar experiments with cohesive silt (Kleinhans *et al.*, 2014a) and in the field (Rinaldi and Darby, 2007). The transport capacity in the channel is so large that the type of erosion does not affect the erosion rate in this set-up. Cohesive blocks are transported as a whole and destroyed rapidly. Even though we do not observe decreased bank erosion with nutshell, we observe that cohesive mats prevent erosion of mud particles with lower velocities under a more gradual slope in the estuary experiments. This suggests that the mild cohesion may reduce channel initiation and incision on bar tops in the experiments, but does not directly confine the estuary laterally.

Bar accretion by mud deposition

Bar accretion is caused by mud deposition on bars. In the experiment without mud supply, the bars are >5 mm below the initial dry estuary margin and are therefore submerged during high tide. In contrast, the bars in the experiment with mud are 3–10 mm higher due to the mud deposits on top of the bars (Figure 2). The bar accretion can be as high as 5 mm. This is clearly visible in Figure 11, where the cumulative surface area below 0 to −0.5 cm is constant for the experiment without mud but changes for the experiments with mud. Moreover, the increase in elevation of the bars is visible in Figure 3, where the 90th percentile of the elevation is higher for the experiments with mud. Visual observations also confirmed that the top of the mudflats on bars changed from intertidal to supratidal (supratidal bar visible in Figures 9a and 9b). This also contributed to the decrease in tidal prism and tidal range, which we will discuss later.

Because mud only settles at very low velocities and shear stresses (Torfs *et al.*, 1996), the places for deposition are different from the situation for sand (dotted lines in Figure 7). During ebb flow, mud is supplied to the system and spreads downstream by river discharge. Mud settling occurs mainly during slack tide due to near-zero flow velocities (below the critical threshold of mud mobility; Figure 7), which occurs near maximum high and maximum low water. At mean and low water levels the flow is concentrated in the channels and mud deposits cannot be preserved here due to high peak velocities (Figure 6b). Figure 7 also shows that peak velocities below the mud mobility threshold only occur at high elevations. Everything that deposits during low-water slack is immediately washed away again during the next flood, whereas deposits during high-water slack are more likely to preserve. During high water, bars are flooded and velocities slow down. Mud settles at these high elevations during slack tide because the water depth is shallow and cannot be resuspended during mean and low water levels.

Peak velocity ratios indicate that mud deposits during high water can be related to flood in the lower and ebb in the upper estuary (Figure 6d). Upstream, the river has a larger influence and therefore ebb asymmetry is observed for peak velocity over a large area. Around the tidal bars in the lower estuary, peak velocity asymmetry is flood dominated (Figure 6d). Duration asymmetry was less pronounced and is therefore not shown. Longer flood durations were observed in small barb

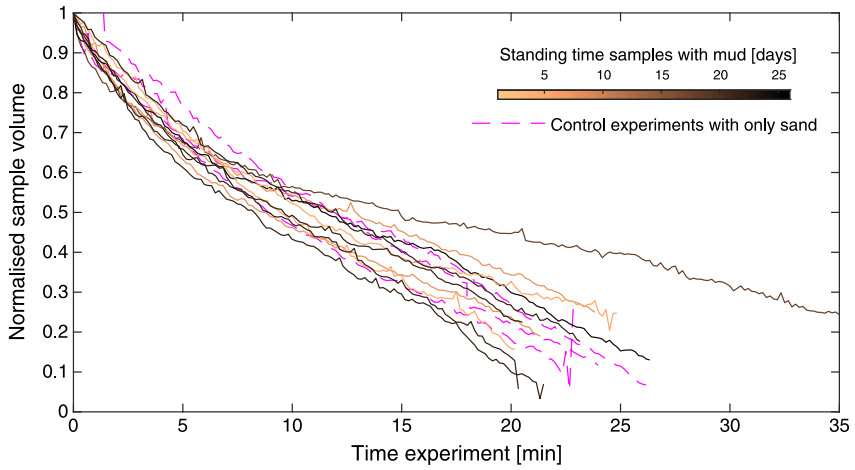

Figure 13. Volume of samples during bank erosion tests over time. Pink colours are control experiments with only sand. Orange-brown colours indicate the standing time of the samples with a mud layer between making the sample and conducting the experiment. There are no differences in observed erosion rates for sediment type or standing time, which implies that bank erosion is not affected by mud. [Colour figure can be viewed at wileyonlinelibrary.com]

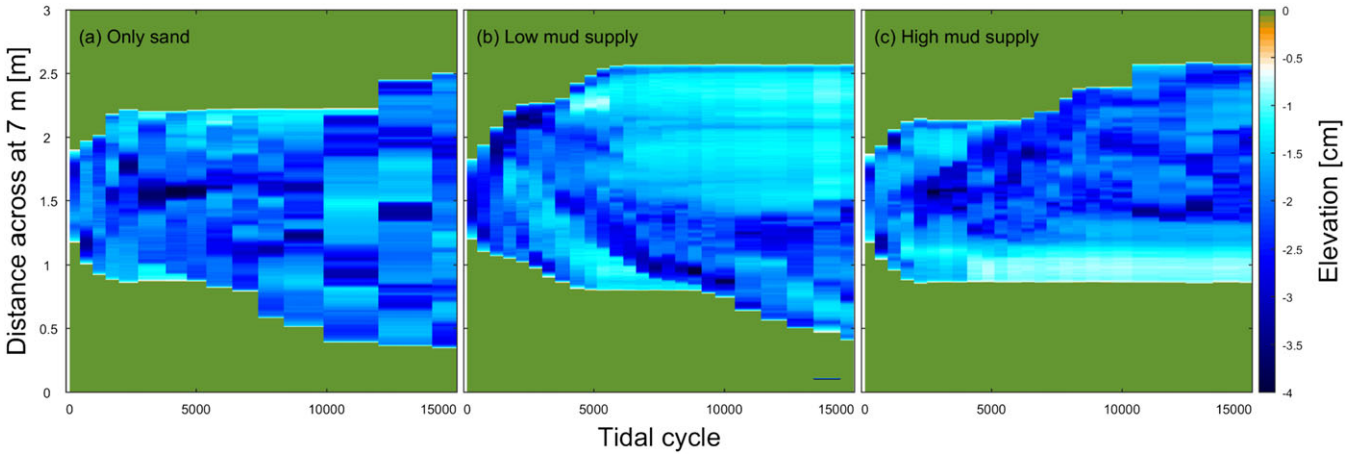

Figure 14. Time-stacks: bathymetric evolution of a cross-section at 7 m over time for the experiment with (a) only sand, (b) a low mud supply and (c) a high mud supply. Cross-sections increase over time. Shallow areas in (b) and (c) are mudflats that prevent the channel migrating in that direction. The temporal resolution of the DEMs in (a) is too low to track the fast channel migration. [Colour figure can be viewed at wileyonlinelibrary.com]

channels that terminate on their landward end; however, clear patterns were hard to identify. It is known that duration asymmetry is especially important for fine sediments, so we assume that most mud is deposited during high-water slack following the flood, with the exception of the most upstream areas. Peak velocity and duration ratios could not be determined in areas where the flow was unidirectional and for supratidal areas.

Mud confines the estuary shape

Deposition of mud on bars and on the sides confines the estuary shape and therefore decreases the width and surface area, especially upstream where there is more mud present (Figures 4 and 10). The effect on widening downstream is limited because less mud is deposited in this part of the estuary. Not only is the width of the estuary confined by mud, but also the total reworked surface area (maximum values in Figure 11). Even though the specific tidal meandering leads to a wider estuary mouth of 2.75 m for the experiment with the high mud supply, compared to 2.1 m and 1.5 m of the other experiments (Figure 2), the surface area of that experiment is smaller than the experiment with only sand (Figures 11a and 11c). The total estuary area without mud increases up to 25 m^2, whereas the area of the experiments with mud cover an area of only 20 m^2 (Figure 11). Surprisingly, the estuary with the high mud supply is roughly the same size as the estuary with low mud supply. This is probably caused by the difference in the geometry of the mouth, which is barely affected by mud and narrower for the experiment with low mud supply. However, we cannot exclude the possibility that this is due to the software error that led to reduced tilting amplitude in the experiment with low mud supply. We expect that under the correct tilting the experiment would have been slightly larger than the one with the high mud supply, but still smaller than the experiment with only sand due to the confinement and filling mechanism.

Mud decreases estuary dynamics

Mud decreases the dynamics of channels and bars. Channels initially migrate and shift rapidly within the estuary (Figure 14), but when mudflats develop the lateral widening of the estuary at the mudflat comes to a halt (Figures 14e and 14f). In the cross-section of the low mud supply, a mudflat developed on the bottom side and for the high mud supply on the top side of Figures 14e and 14f. The migration in the experiment without mud is sometimes so fast that not enough DEMs were made to follow the channel displacement in the time-stack (Figure 14d). Observations with a higher temporal resolution from the overhead imagery for sand only show that channels remain active and rework bars in specific zones over the entire length of the experiment (Leuven *et al.*, 2018a).

The width changes of the estuary in Figure 4 also shows decreasing dynamics due to mud. For all experiments it holds that initially the estuary largely widens (wider spaced lines) and the widening rate decreases over time (closer spaced lines) as the estuary dimensions get closer to equilibrium conditions (Figure 4). This decrease in change is more pronounced for the experiments with mud because the mud has confined the estuary, which is then also sooner close to equilibrium with reduced dynamics (Figure 5).

The addition of mud significantly decreases erosion rates within the estuary. Without mud the estuary exported 0.25 m^3 of sediment in total and with mud only approximately 0.17 m^3 (Figure 5). The export is essentially continuous and there are no clear signs of net import. All data so far suggest that the created system is an exclusively exporting system; however, visual observations confirmed landward sand movement during flood. This transport was apparently not enough to counteract export. Variations in the general trend of the lines in Figure 5 are due to inaccuracies of the DEMs. Similar to the analysis of the surface area, the experiments do not show any evidence of decreasing sediment export for higher mud concentration. Both Experiments 2 and 3 have similar exported sediment volumes and surface areas (Figure 5), even though the shape of the mouth is especially different. Due to the tilting amplitude error, the export in the experiment with low mud supply may have been slightly smaller than expected.

Discussion

In this section, we will first describe the two effects of mud that impact the morphological evolution of the system. Next, we will discuss the implications of our findings on the understanding of natural systems, followed by a discussion of the novelty and contribution of this research to the current state of physical experiments simulating estuaries and experiments with mud.

Cohesive effect of mud

Two effects of mud were identified to cause morphological differences between estuaries with and without mud. The first effect is the minor apparent cohesion that increases over time because nutshell grains stick together the longer they are in the experiment. The grains form a mat-like structure. These cohesive effects cause small cliffs to form and lead to different bank erosion processes that include oversteepening and mass failures (Rinaldi and Darby, 2007), in contrast to more gentle slopes and gradual erosion for sand. However, auxiliary bank erosion tests did not show a significant effect on erosion rate (Figure 13). Small effects on the erosion rate are visually observed under low velocities on more gentle slopes.

Apparent cohesion can also be created by vegetation (Tal and Paola, 2007). Roots and extracellular polymeric substances (EPS) can stabilise banks similarly to cohesive sediment. However, it is still unclear whether vegetation and mud together provide significant cohesion in tidal systems or only reduce the flood storage as discussed below (De Haas *et al.*, 2018). On the one hand, vegetation and mud might settle in the same locations and therefore an additional strengthening effect might be limited. On the other hand, vegetation also reduces flow velocities by creating friction, which might increase significant amounts of mud deposition and more vegetation settling. Further investigation and experimentation of mud in combination with vegetation is part of our future work.

Filling effect of mud

The second, perhaps more important effect of mud is to fill space and reduce the tidal prism and the possibility for bar splitting. The results showed that mud deposits further increase the elevation of areas that are already relatively high in elevation. For example, sandbars become higher when mud is supplied to the system (Figure 3). This result agrees with earlier work by numerical modelling of mud in estuaries (Braat *et al.*, 2017). Like the cohesive effects, this deposition contributes to confining the estuary but additionally limits the tidal prism (Figure 15). The prism is reduced because less water can flow through a cross-section as part of the cross-section is now filled with mud. This effect is clearly visible in the upstream part of the estuaries where most mud is deposited. In Figure 15 the local tidal prism for the experiment with only sand continues to grow up to a local tidal prism of 0.07 m^3 passing the 10 m cross-section. For the experiment with low mud supply, we also observe a growth in tidal prism, but less strong. The prism at 10 m grows up to 0.053 m^3. For the high-mud-supply experiment, we even observe a reduction of the tidal prism over time in the upper part of the estuary. The final local tidal prism at 10 m is 0.043 m^3 and only 60% compared to the tidal prism for only sand. Wobbles in these lines can be correlated with individual bends that influence the width of the estuary.

A surprising insight from these experiments is therefore the different effect of mud sedimentation in rivers and estuaries. In contrast to rivers where floodplain sedimentation causes the channel to deepen to accommodate the same river discharge through a cross-section (Tal and Paola, 2007), in estuaries the tidal prism adapts to the decrease in cross-sectional area. With a decrease in tidal prism, sediment transport also decreases.

In addition to the filling mechanism, water level decrease also contributes to tidal prism decrease over time. Because we do not have measurements of water levels, we could only visually observe a decrease in tidal range with time. A fixed high and low water level was assumed along the flume and in time to calculate tidal prism and is, therefore, an overestimation. The prism reduction effect we describe is therefore probably stronger than visualised in Figure 15. Tidal prism was calculated along the flume which we define as local tidal prism: the volume between low and high water upstream of this point (Figure 15). In addition to the decrease in tidal prism by the filling effect of mud, we assume the water level decreases by increased friction in the estuary due to the filling and the development of more complicated bars and channels. According to Dalrymple and Choi (2007), this means that the estuary becomes more hyposynchronous: the friction of the bottom increases and the convergence is less strong, leading to a stronger decrease in tidal range towards the tidal limit. This is in accordance with the positive feedback identified by De Haas *et al.* (2018): the formation of shoals simulates the deposition of more mud leading to a growth of supratidal areas (reduction of intertidal area), further stimulating the growth of new intertidal areas, ultimately increasing friction and reducing tidal prism. This mechanism predicts that, with enough sand and mud available, all estuaries eventually fill up (De Haas *et al.*, 2018).

Implications for understanding natural systems

The depositional patterns of mud match the classical patterns described by Dalrymple *et al.* (1992) and Dalrymple and Choi (2007). Mudflats are flanking the estuary and are depositing on bars, while the seaward part is largely free of mud (Dalrymple and Choi, 2007). In addition, when the

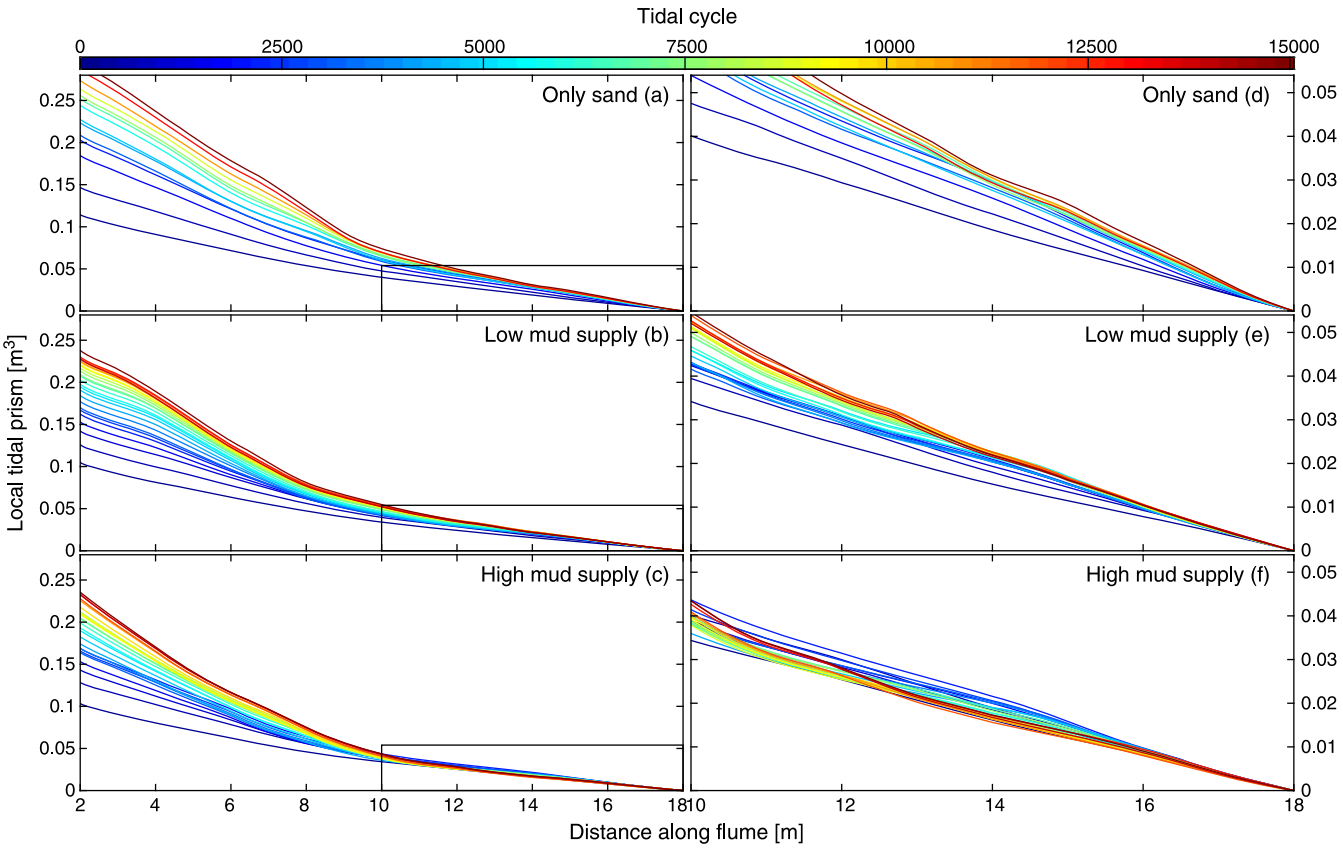

Figure 15. Locally defined tidal prism along the estuary at different moments in time for (a) the experiment with only sand, (b) the experiment with a low mud supply and (c) the experiment with a high mud supply. (d–f) Zoomed in on the upstream region of the estuaries. Tidal prism increases in the upstream region with high mud supply. [Colour figure can be viewed at wileyonlinelibrary.com]

results are compared to data from real-world estuaries, we note that for many real-world estuaries the relative extent of mudflats is larger upstream, similar to our experiments: Western Scheldt (McLaren, 1993, 1994), Ems-Dollard (Van Heuvel, 1991), Dovey (Baas *et al.*, 2008), Severn (Allen, 1987) and the Salmon River estuary (Dalrymple and Choi, 2007). This trend was also observed in numerical models (Braat *et al.*, 2017; Lokhorst *et al.*, 2018). Since the field data support the experimental results, the experiment can help us understand how the mudflats in the system are formed. Bars in estuaries are mostly built by sand; only when they get more stable does mud start settling on top of the bars. The preferential settling of mud upstream is not due to supply location, because the mud is transported through the whole estuary and also ends up in the ebb delta. Fewer mud deposits downstream are due to the larger velocities and larger dynamics in the lower estuary. We expect that a marine supply would lead to a similar spatial distribution between the mouth and the upper tidal limit.

When bars increase in elevation because of mudflat accretion, they can change from intertidal to supratidal due to the filling effect and decrease in water level. This has important implications for marsh formation. These areas could potentially be a starting point where pioneer marsh species can find their window of opportunity (Cao *et al.*, 2017; De Haas *et al.*, 2018). This was recently also concluded in a numerical modelling study of estuaries with mud and vegetation (Lokhorst *et al.*, 2018). An important question related to vegetation and mud settling is whether the vegetation supports mud settling, or the other way around, or both. Showing that we can create mudflats in these experiments partly solved this chicken-or-egg problem. At least vegetation is not necessary for extensive mudflats or to increase the elevation of tidal bars. In the Western Scheldt, elevation of bars has been increasing over past years and is often considered an undesired consequence of dredging and dumping (Cleveringa, 2013; De Vet *et al.*, 2017). However, this study shows that this trend can also partly be attributed to changes in mud supply either by natural or anthropogenic changes.

Besides the increase in bar height, the results showed that mud supply also influences the width, size and dynamics of the estuary morphology. Due to the filling mechanism and reduction in tidal prism, the estuary becomes more confined. The reduction in width and size was also observed in numerical models with mud (Braat *et al.*, 2017). Similar to the experiments, the dynamics of channels and bars also decreased in models with mud compared to estuaries with only sand. Observing the same trends with both methods strengthens the certainty of these findings.

However, some differences are also observed between the models and the experiments. The models (Braat *et al.*, 2017) show predominantly deposits on the sides, while in the experiments most deposits are on bars instead of on the sides. This probably relates to the balance between the initial and boundary conditions. In the model, there is initial import into the system, while in the experiments the estuary is mostly exporting, despite the filling mechanism discussed earlier. Because the experiments are widening over time, mud is rarely deposited on the sides. An alternative hypothesis is that varying discharge is necessary to form flats on the sides, as seen for floodplain formation in river experiments (Van Dijk *et al.*, 2013). The initial horizontal bed is not flooded during high water for mud to deposit as overbank deposits. We expect that the confining effect of the estuary would be greater if this type of deposit formed. This could be achieved by adding spring and neap tides, for example. Other similarities with river experiments were found in strengthening of banks, decrease in

meandering and a decrease in chutes (Van Dijk *et al.*, 2013). However, since the prism adapts to the cross-sections, we do not observe deeper channels as for rivers where the discharge through the cross-section is forced.

Numerical models indicate that confinement of the estuary by mud can lead to a dynamic equilibrium (Braat *et al.*, 2017), but we did not find such equilibrium in the experiments, although the equilibrium for experiments with mud is probably closer than for only sand (Figure 5). We hypothesise that the experiments could also reach an equilibrium if filling continues and friction would further increase, decreasing the tidal prism and tidal amplitude. If this is true, this would have important implications for estuary management, since altering the system by dredging might constantly bring the estuary out of equilibrium. If the equilibrium dimensions of an estuary are known, bringing the estuary closer towards these dimensions will likely decrease the dynamics and will make maintenance of the shipping channel easier, while bringing the estuary out of equilibrium will only increase dynamics and will make maintenance of shipping fairways more difficult.

While high mud concentrations are often seen as negative because of fluid mud, decreasing light penetration and silting up of harbours; some mud is important for ecology. Muddy areas are often the most biologically active areas of the estuary and an important part of the ecosystem (Costanza *et al.*, 1993). These ecosystems can be largely affected by changes in mud supply concentration. The results show that if mud were absent intertidal flats would be lower and might drown species that prefer high intertidal or supratidal regions. Many benthic species also prefer a muddy substrate (Bouma *et al.*, 2005). Results also suggest that if mudflats are absent the estuary will expand faster, which might affect surrounding areas if there are no dikes bordering the estuary.

Novelty of mud in tidal experiments

The results showed an improvement in the methodology of conducting tidal experiments. Continuous dynamics were obtained with dynamic ebb- and flood-dominated channels that are typical for tidal systems. These channels were previously described by Van Veen (1950) and are essential for natural estuarine behaviour. It had been somewhat difficult to maintain dynamics in experiments in the past (Kleinhans *et al.*, 2012; Vlaswinkel and Cantelli, 2011), but these experiments show dynamic channels without any extra trigger or irregular forcing. This is because the Metronome was successful in achieving sediment mobility along the whole estuary in both flow directions.

Of additional interest is that the shape and patterns are self-formed. Until now, the shape of the estuary was often imposed especially for numerical models (Hibma *et al.*, 2003; Van der Wegen and Roelvink, 2008), but also for experiments (Tambroni *et al.*, 2005). The final shape of the estuary is a self-formed exponential shape with some deviations (Figure 4). It is widely accepted that an exponential shape is the natural equilibrium planform of most natural estuaries (Lanzoni and Seminara, 2002; Savenije, 2015). However, observations in natural systems show that the width of estuaries can be rather irregular than ideal exponential (Leuven *et al.*, 2018b). The locations where the estuary is wider than ideal are those where bars occur in natural systems, which is consistent with observations in the experiments (Leuven *et al.*, 2018a). These bars are intertidal areas and, because flow velocity on the bars is low, they are also the places where mud is likely to settle when available. Therefore, the outline of the estuaries is a relevant indicator for the locations of mudflats, which also translates into predictable depth distributions (Leuven *et al.*, 2018c).

Idealised experimental studies like this are useful to get an understanding of the main processes that are involved in the morphological evolution of estuaries. These processes are hard to isolate from field data, and data are generally sparse. However, detailed results should be interpreted with caution as detail in the natural morphology might be hampered by scale effects, such as the occurrence of scour holes (Kleinhans *et al.*, 2017a), or are influenced by processes that were neglected, such as additional tidal components, inherited hard substrates and salinity. These effects cannot presently be accounted for in large-scale system experiments.

A side effect of solving the mobility scaling problem with the tilting flume is that the water-level variations are now caused by the flow instead of flow caused by water-level variations. This means that the water level is no longer a simple function of the tides but a complex result of local friction and the wave of water going through the system as the flume tilts, while the typical phase relations for estuaries between flow and water level are lost (Kleinhans *et al.*, 2017b).

Using nutshell as a proxy for mud also imposes limitations. The cohesive properties could not exactly be simulated at scale, because the degradation of the mud was poorly constrained as it depends on the temperature of the room, water, possibly inundation duration and the total time it has been in the flume. As a consequence, we believe that the cohesiveness of recently deposited nutshell was too low, whereas it was too high for nutshell that had been in the flume for over 10 000 cycles. Since these older deposits were rarely subjected to large velocities, the effect on the final results was minimal, although perhaps the bars in the centre of the estuary might have been over-stabilised.

On the other hand, numerical models often also apply similar simplifications, such as ignoring multiple tidal components, multiple grain sizes, salinity and three-dimensional velocity calculations, especially for large timescales. Even though scaling issues are absent, there are uncertainties in the physical representation of processes in models. To quantify these uncertainties and assess their effects, more studies with analogue experiments are desirable. The contribution of the present experiments is to complement the approach of numerical modelling.

Conclusions

The aim of the present research was to examine the effects of mud on the shape and dynamics of estuaries. Experiments in a novel tilting tidal flume – the Metronome – show that mudflat formation confines the morphology of the estuary. The main effect of mud is that it deposits in areas that would not otherwise be filled with sand and therefore decreases the local tidal prism, which, in turn, reduces the migration of channels and large-scale widening of the estuary. As a result, the estuary becomes more confined as the width remains smaller, especially upstream, and total surface area of the estuary remains smaller with mud compared to only sand. Cohesive effects are surprisingly minor compared to the important role of cohesive floodplains on river patterns.

The second major finding was that mud increases the elevation of the bars and can transform bar surfaces from intertidal to supratidal. Bars and channels migrate slower and the estuary exports less sediment when mud is added to the system. Mud has a non-uniform spatial distribution along the estuary: more mud deposits upstream and therefore more morphological effects of the mud are observed upstream than

downstream. In more detail, we found that mud is mostly deposited at intertidal bed elevations but preservation over time increases for higher elevations.

Acknowledgments

This research was funded by the Domain of Applied and Engineering Sciences TTW (grant Vici 016.140.316/13710 to MK) of the Netherlands Organisation for Scientific Research (NWO) and is part of the PhD project of LB. We would like to thank the technical staff of Physical Geography for their support, especially Arjan van Eijk, Chris Roosendaal and Marcel van Maarseveen for the daily problem solving and creative inventions. Wout van Dijk, Marcio Boechat Albernaz and Anne Baar are acknowledged for interesting discussions and comments on the manuscript. We gratefully acknowledge two anonymous reviewers for their constructive comments.

The authors contributed in the following proportions to concept and design, experiments, analysis and conclusions and manuscript preparation: LB (55, 65, 70, 80), JL (10, 30, 10, 0), IL (0, 5, 5, 0) and MK (35, 0, 15, 20).

References

Allen J. R. L. 1987. Reworking of muddy intertidal sediments in the Severn estuary, southwestern UK: A preliminary survey. *Sedimentary Geology* **50**(1–3): 1–23. https://doi.org/10.1016/0037-0738(87)90026-1.

Ashmore P. E. 1991. How do gravel-bed rivers braid *Canadian Journal of Earth Sciences* **28**(3): 326–341. https://doi.org/10.1139/e91-030.

Baar A. W., de Smit J., Uijttewaal W. S. J., Kleinhans M. G. 2018. Sediment transport of fine sand to fine gravel on transverse bed slopes in rotating annular flume experiments. *Water Resources Research* **54**(1): 19–45. https://doi.org/10.1002/2017WR020604.

Baas J. H., Jago C., Macklin M., Team C C. C. R. 2008. The river–estuarine transition zone (RETZ) of the Afon Dyfi (west Wales) as test bed for sediment transfer between river catchments and coastal environments. In *BSRG 2008*, Liverpool: UK; 14–17.

Baumgardner S. E. 2016. *Quantifying Galloway: fluvial, tidal and wave influence on experimental and field deltas*. PhD thesis, University of Minnesota.

Bouma H., de Jong D. J., Twisk F., Wolfstein K. Zoute wateren ecotopenstelsel (zes.1), Ministerie van Verkeer en Waterstaat Rijkswaterstaat, Middelburg, 2005.

Braat L., van Kessel T., Leuven J. R. F. W., Kleinhans M. G. 2017. Effects of mud supply on large-scale estuary morphology and development over centuries to millennia. *Earth Surface Dynamics* **5**(4): 617–652. https://doi.org/10.5194/esurf-5-617-2017.

Braudrick C. A., Dietrich W. E., Leverich G. T., Sklar L. S. 2009. Experimental evidence for the conditions necessary to sustain meandering in coarse-bedded rivers. *Proceedings of the National Academy of Sciences* **106**(40): 16936–16941. https://doi.org/10.1073/pnas.0909417106.

Cao H., Zhu Z., Balke T., Zhang L., Bouma T. J. 2017. Effects of sediment disturbance regimes on Spartina seedling establishment: implications for salt marsh creation and restoration. *Limnology and Oceanography* **63**(2): 647–659. https://doi.org/10.1002/lno.10657.

Cleveringa J. 2013. Ontwikkeling mesoschaal westerschelde [fact sheets]. Basisrapport kleinschalige ontwikkeling K-16 I/RA/11387/13.083/GVH, VNSC, International Marine and Dredging Consultants/Deltares/Svaek Hydraulics BV/ARCADIS Nederland BV.

Costanza R., Kemp W. M., Boynton W. R. 1993. Predictability, scale, and biodiversity in coastal and estuarine ecosystems: Implications for management. *Ambio* **22**(2–3): 88–96.

Dalrymple R. W., Choi K. 2007. Morphologic and facies trends through the fluvial–marine transition in tide-dominated depositional systems: A schematic framework for environmental and sequence-stratigraphic interpretation. *Earth-Science Reviews* **81**(3): 135–174. https://doi.org/10.1016/j.earscirev.2006.10.002.

Dalrymple R. W., Zaitlin B. A., Boyd R. 1992. Estuarine facies models: Conceptual basis and stratigraphic implications: Perspective. *Journal of Sedimentary Research* **62**(6): 1130–1146. https://doi.org/10.1306/D4267A69-2B26-11D7-8648000102C1865D.

Dam G., van der Wegen M., Labeur R. J., Roelvink D. 2016. Modeling centuries of estuarine morphodynamics in the Western Scheldt estuary. *Geophysical Research Letters* **43**(8): 3839–3847. https://doi.org/10.1002/2015GL066725.

Dam G., van der Wegen M., Roelvink D. 2013. *Long-term performance of process-based models in estuaries*, *In* Proceedings of the Coastal Dynamics Conference 2013: Archachon, France, 409–420.

De Haas T., Pierik H. J., van der Spek A. J. F., Cohen K. M., van Maanen B. 2018. Holocene evolution of tidal systems in the Netherlands: Effects of rivers, coastal boundary conditions, eco-engineering species, inherited relief and human interference. *Earth-Science Reviews* **177**: 139–163. https://doi.org/10.1016/j.earscirev.2017.10.006.

De Vet P. L. M., van Prooijen B. C., Wang Z. B. 2017. The differences in morphological development between the intertidal flats of the Eastern and Western Scheldt. *Geomorphology* **281**: 31–42. https://doi.org/10.1016/j.geomorph.2016.12.031.

Dijkstra J., van Kessel T., van Maren B., Spiteri C., Stolte W. Setup of an effect-chain model for the Eems-Dollard, Technical Report Technical Report 1202298-000-ZKS-0002, Deltares Delft, Netherlands, 2011.

Friedkin J. F. A laboratory study of the meandering of alluvial rivers, Technical Report Technical report, War Department, US Army Corps of Engineers, 1945.

Ganti V., Chadwick A. J., Hassenruck-Gudipati H. J., Fuller B. M., Lamb M. P. 2016. Experimental river delta size set by multiple floods and backwater hydrodynamics. *Science Advances* **2**(5): e1501768. https://doi.org/10.1126/sciadv.1501768.

Grimaud J-L, Paola C., Ellis C. 2017. Competition between uplift and transverse sedimentation in an experimental delta. *Journal of Geophysical Research: Earth Surface* **122**(7): 1339–1354. https://doi.org/10.1002/2017JF004239.

Hibma A., de Vriend H. J., Stive M. J. F. 2003. Numerical modelling of shoal pattern formation in well-mixed elongated estuaries. *Estuarine, Coastal and Shelf Science* **57**(5): 981–991. https://doi.org/10.1016/S0272-7714(03)00004-0.

Hoyal D. C. J. D., Sheets B. A. 2009. Morphodynamic evolution of experimental cohesive deltas. *Journal of Geophysical Research: Earth Surface* **114**(F2). https://doi.org/10.1029/2007JF000882.

Hughes S. A. 1993. *Physical Models and Laboratory Techniques in Coastal Engineering*, Vol. 7. World Scientific: Singapore.

Kleinhans M. G. 2010. Sorting out river channel patterns. *Progress in Physical Geography* **34**(3): 287–326. https://doi.org/10.1029/2005WR004674.

Kleinhans M. G., Leuven J. R. F. W., Braat L., Baar A. W. 2017a. Scour holes and ripples occur below the hydraulic smooth to rough transition of movable beds. *Sedimentology* **64**(5): 1381–1401. https://doi.org/10.1111/sed.12358.

Kleinhans M. G., Terwisscha van Scheltinga R., van der Vegt M., Markies H. 2015. Turning the tide: Growth and dynamics of a tidal basin and inlet in experiments. *Journal of Geophysical Research: Earth Surface* **120**(1): 95–119. https://doi.org/10.1002/2014JF003127.

Kleinhans M. G., van Dijk W. M., van de Lageweg W. I., Hoyal D. C. J. D., Markies H., van Maarseveen M., Roosendaal C., van Weesep W., van Breemen D., Hoendervoogt R., Cheshier N. 2014a. Quantifiable effectiveness of experimental scaling of river- and delta morphodynamics and stratigraphy. *Earth-Science Reviews* **133**: 43–61. https://doi.org/10.1016/j.earscirev.2014.03.001.

Kleinhans M. G., Van Rosmalen T. M., Roosendaal C., van der Vegt M. 2014b. Turning the tide: Mutually evasive ebb- and flood-dominant channels and bars in an experimental estuary. *Advances in Geosciences* **39**: 21–26. https://doi.org/10.5194/adgeo-39-21-2014.

Kleinhans M. G., van der Vegt M., Leuven J. R. F. W., Braat L., Markies H., Simmelink A., Roosendaal C., Eijk A., Vrijbergen P., van Maarseveen M. 2017b. Turning the tide: Comparison of tidal flow by periodic sea level fluctuation and by periodic bed tilting in scaled landscape experiments of estuaries. *Earth Surface Dynamics* **5**(4): 731–756. https://doi.org/10.5194/esurf-5-731-2017.

Kleinhans M. G., van der Vegt M., Terwisscha van Scheltinga R., Baar A. W., Markies H. 2012. Turning the tide: Experimental creation of tidal channel networks and ebb deltas. *Netherlands Journal of Geosciences* **91**(3): 311–323. https://doi.org/10.1017/S0016774600000469.

Lanzoni S., Seminara G. 2002. Long-term evolution and morphodynamic equilibrium of tidal channels. *Journal of Geophysical Research: Oceans* **107**(C1). https://doi.org/10.1029/2000JC000468.

Le Hir P., Ficht A., Jacinto R. S., Lesueur P., Dupont J.-P., Lafite R., Brenon I., Thouvenin B., Cugier P. 2001. Fine sediment transport and accumulations at the mouth of the Seine estuary (France). *Estuaries* **24**(6): 950–963. https://doi.org/10.2307/1353009.

Leuven J. R. F. W., Braat L., van Dijk W. M., de Haas T., van Onselen E. P., Ruessink B. G., Kleinhans M. G. 2018a. Growing forced bars determine non-ideal estuary planform. *Journal of Geophysical Research: Earth Surface, early view*. https://doi.org/10.1029/2018JF004718.

Leuven J. R. F. W., de Haas T., Braat L., Kleinhans M. G. 2018b. Topographic forcing of tidal sand bar patterns for irregular estuary planforms. *Earth Surface Processes and Landforms* **43**(1): 172–186. https://doi.org/10.1002/esp.4166.

Leuven J. R. F. W., Selakovic S., Kleinhans M. G. 2018c. Morphology of bar-built estuaries: Relation between planform shape and depth distribution. *Earth Surface Dynamics* **6**(3): 763–778. https://doi.org/10.5194/esurf-6-763-2018.

Lokhorst I. R., Braat L., Leuven J. R. F. W., Baar A. W., van Oorschot M., Selakovic S., Kleinhans M. G. 2018. Morphological effects of vegetation on the fluvial–tidal transition in Holocene estuaries. *Earth Surface Dynamics* **6**(4): 242–254. https://doi.org/10.5194/esurf-6-883-2018.

McLaren P. Patterns of sediment transport in the western part of the Westerschelde, Technical Report Technical report, GeoSea Consulting Cambridge, UK, 1993.

McLaren P. Sediment transport in the Westerschelde between Baarland and Rupelmonde, Technical Report Technical report, GeoSea Consulting Cambridge, UK, 1994.

Moore R. D., Wolf J., Souza A. J., Flint S. S. 2009. Morphological evolution of the dee estuary, eastern Irish Sea, UK: A tidal asymmetry approach. *Geomorphology* **103**(4): 588–596. https://doi.org/10.1016/j.geomorph.2008.08.003.

Paola C., Straub K., Mohrig D., Reinhardt L. 2009. The unreasonable effectiveness of stratigraphic and geomorphic experiments. *Earth-Science Reviews* **97**(1): 1–43. https://doi.org/10.1016/j.earscirev.2009.05.003.

Peakall J., Ashworth P. J., Best J. L. 1996. Physical modelling in fluvial geomorphology: Principles, applications and unresolved issues. In *The Scientific Nature of Geomorphology*, Rhodes BL, Thorn CE (eds), Wiley: Chichester, UK; 221–253.

Peakall J., Ashworth P. J., Best J. L. 2007. Meander-bend evolution, alluvial architecture, and the role of cohesion in sinuous river channels: A flume study. *Journal of Sedimentary Research* **77**(3): 197–212. https://doi.org/10.2110/jsr.2007.017.

Reynolds O. On certain laws relating to the regime of rivers and estuaries and on the possibility of experiments on a small scale, Technical Report Report of the British Association, 1887.

Reynolds O. Report of the committee appointed to investigate the action of waves and currents on the beds and foreshores of estuaries by means of working models, Technical Report Report of the British Association, 1889.

Reynolds O. Third report of the committee appointed to investigate the action of waves and currents on the beds and foreshores of estuaries by means of working models, Technical Report Report of the British Association, 1891.

Ridgway J., Shimmield G. 2002. Estuaries as repositories of historical contamination and their impact on shelf seas. *Estuarine, Coastal and Shelf Science* **55**(6): 903–928. https://doi.org/10.1006/ecss.2002.1035.

Rinaldi M., Darby S. E. 2007. Modelling river-bank-erosion processes and mass failure mechanisms: Progress towards fully coupled simulations. *Developments in Earth Surface Processes* **11**: 213–239. https://doi.org/10.1016/S0928-2025(07)11126-3.

Savenije H. H. G. 2015. Prediction in ungauged estuaries: An integrated theory. *Water Resources Research* **51**(4): 2464–2476. https://doi.org/10.1002/2015WR016936.

Smith A. L. 1909. Delta experiments. *Bulletin of the American Geographical Society* **41**(12): 729–742. https://doi.org/10.2307/199425.

Stefanon L., Carniello L., D'Alpaos A., Lanzoni S. 2010. Experimental analysis of tidal network growth and development. *Continental Shelf Research* **30**(8): 950–962. https://doi.org/10.1016/j.csr.2009.08.018.

Tal M., Paola C. 2007. Dynamic single-thread channels maintained by the interaction of flow and vegetation. *Geology* **35**(4): 347–350. https://doi.org/10.1130/G23260A.1.

Tambroni N., Bolla Pittaluga M., Seminara G. 2005. Laboratory observations of the morphodynamic evolution of tidal channels and tidal inlets. *Journal of Geophysical Research: Earth Surface* **110**(F4). https://doi.org/10.1029/2004JF000243.

Torfs H., Mitchener H., Huysentruyt H., Toorman E. 1996. Settling and consolidation of mud/sand mixtures. *Coastal Engineering* **29**: 27–45. https://doi.org/10.1016/S0378-3839(96)00013-0.

Van Dijk W. M., van de Lageweg W. I., Kleinhans M. G. 2013. Formation of a cohesive floodplain in a dynamic experimental meandering river. *Earth Surface Processes and Landforms* **38**(13): 1550–1565. https://doi.org/10.1002/esp.3400.

Van Heuvel T. Sedimenttransport in het eems-dollard estuarium, volgens de method McLaren, Technical Report Nota GWWS-91.002, Rijkswaterstaat, dienst Getijdewateren, 1991.

Van Kessel T., Vanlede J., de Kok J. 2011. Development of a mud transport model for the Scheldt estuary. *Continental Shelf Research* **31**(10): S165—S181. https://doi.org/10.1016/j.csr.2010.12.006.

Van Maren D. S., Oost A. P., Wang Z. B., Vos P. C. 2016. The effect of land reclamations and sediment extraction on the suspended sediment concentration in the ems estuary. *Marine Geology* **376**: 147–157. https://doi.org/10.1016/j.margeo.2016.03.007.

Van Maren D.S., Van Kessel T., Cronin K., Sittoni L. 2015. The impact of channel deepening and dredging on estuarine sediment concentration. *Continental Shelf Research* **95**: 1–14. https://doi.org/10.1016/j.csr.2014.12.010.

Van Veen J. 1950. Ebb and flood channel systems in the Netherlands tidal waters. *Journal of the Royal Dutch Geographical Society* **67**: 303–325. https://doi.org/10.2112/04-0394.1.

Van de Lageweg W. I., van Dijk W. M., Box D., Kleinhans M. G. 2016. Archimetrics: A quantitative tool to predict three-dimensional meander belt sandbody heterogeneity. *Depositional Record* **2**(1): 22–46. https://doi.org/10.1002/dep2.12.

Van der Wegen M. 2013. Numerical modeling of the impact of sea level rise on tidal basin morphodynamics. *Journal of Geophysical Research: Earth Surface* **118**(2): 447–460. https://doi.org/10.1002/jgrf.20034.

Van der Wegen M., Roelvink J. 2008. Long-term morphodynamic evolution of a tidal embayment using a two-dimensional, process-based model. *Journal of Geophysical Research: Oceans* **113**(C3). https://doi.org/10.1029/2006JC003983.

Van der Wegen M., Roelvink J. 2012. Reproduction of estuarine bathymetry by means of a process-based model: Western Scheldt case study, the Netherlands. *Geomorphology* **179**: 152–167. https://doi.org/10.1016/j.geomorph.2012.08.007.

Van der Wegen M., Wang Z. B., Savenije H. H. G., Roelvink J. 2008. Long-term morphodynamic evolution and energy dissipation in a coastal plain, tidal embayment. *Journal of Geophysical Research: Earth Surface* **113**(F3). https://doi.org/10.1029/2007JF000898.

Vlaswinkel B. M., Cantelli A. 2011. Geometric characteristics and evolution of a tidal channel network in experimental setting. *Earth Surface Processes and Landforms* **36**(6): 739–752. https://doi.org/10.1002/esp.2099.

Supporting Information

Supporting information may be found in the online version of this article.

